Original Article

Cephalalgia
An International Journal of Headache

International Headache Society

Cephalalgia
2021, Vol. 41(1) 17–32


Article reuse guidelines:
sagepub.com/journals-permissions
DOI: 10.1177/0333102420970507
journals.sagepub.com/home/cep
SAGE

Combined onabotulinumtoxinA/atogepant treatment blocks activation/sensitization of high-threshold and wide-dynamic range neurons

Agustin Melo-Carrillo[1,2], Andrew M Strassman[1,2], Aaron J Schain[1,2], Aubrey Manack Adams[3], Mitchell F Brin[3,4] and Rami Burstein[1,2]

Abstract

Background: OnabotulinumtoxinA and agents that block calcitonin gene–receptor peptide action have both been found to have anti-migraine effects, but they inhibit different populations of meningeal nociceptors. We therefore tested the effects of combined treatment with onabotulinumtoxinA and the calcitonin gene–receptor peptide antagonist atogepant on activation/sensitization of trigeminovascular neurons by cortical spreading depression.

Material and methods: Single-unit recordings were obtained of high-threshold and wide-dynamic-range neurons in the spinal trigeminal nucleus, and cortical spreading depression was then induced in anesthetized rats that had received scalp injections of onabotulinumtoxinA 7 days earlier and intravenous atogepant infusion 1 h earlier. The control group received scalp saline injections and intravenous vehicle infusion.

Results: OnabotulinumtoxinA/atogepant pretreatment prevented cortical spreading depression-induced activation and sensitization in both populations (control: Activation in 80% of high-threshold and 70% of wide-dynamic-range neurons, sensitization in 80% of high-threshold and 60% of wide-dynamic-range neurons; treatment: activation in 10% of high-threshold and 0% of wide-dynamic-range neurons, sensitization in 0% of high-threshold and 5% of wide-dynamic-range neurons).

Discussion: We propose that the robust inhibition of high-threshold and wide-dynamic-range neurons by the combination treatment was achieved through dual blockade of the Aδ and C classes of meningeal nociceptors. Combination therapy that inhibits meningeal C-fibers and prevents calcitonin gene–receptor peptide from activating its receptors on Aδ-meningeal nociceptors may be more effective than a monotherapy in reducing migraine days per month in patients with chronic migraine.

Keywords

Migraine, headache, trigeminal, cortical spreading depression, CGRP, meningeal nociceptor

Date received: 11 August 2020; revised: 3 September 2020; 24 September 2020; accepted: 1 October 2020

Introduction

Since its discovery in the early 1980s (1), the trigeminovascular pathway has been viewed as a single anatomical entity, consisting of peripheral trigeminovascular neurons (also called meningeal nociceptors) that carry nociceptive signals from the meninges to the spinal trigeminal nucleus (STN), central trigeminovascular neurons in the STN that receive nociceptive and non-nociceptive signals from the meninges as well

[1]Department of Anesthesia, Critical Care and Pain Medicine, Beth Israel Deaconess Medical Center, Boston, MA, USA
[2]Department of Anesthesia, Harvard Medical School, Boston, MA, USA
[3]Allergan, an AbbVie Company, Irvine, CA, USA
[4]University of California, Irvine, Irvine, CA, USA

Corresponding author:
Rami Burstein, Department of Anesthesia, Critical Care and Pain Medicine, Beth Israel Deaconess Medical Center, CLS-649, 3 Blackfan Circle, Boston, MA 02215, USA.
Email: rburstei@bidmc.harvard.edu

as other cranial and pericranial organs and tissues and transfer them to the sensory thalamus, and central trigeminovascular neurons in the posterior and ventral posteromedial thalamic nuclei that transmit the sensory information they receive to multiple cortical areas (2–4). While anatomically correct, this simplistic description often disregards the physiological complexity of this pathway, attributable to the fact that each of these components consists of subpopulations of neurons that differ in their physiological characteristics and sensory response properties (5). The peripheral component consists of myelinated Aδ fiber and unmyelinated C-fiber neurons, two classes of nociceptors that exhibit fundamental differences in their membrane receptors and ion channels, neuropeptide/neurotransmitter content, response properties to different intensities, durations, and modes of stimuli, and projection targets in the dorsal horn (6–8). The central component in the STN consists of high-threshold (HT) and wide-dynamic range (WDR) neurons; two classes of nociceptive neurons thought of playing different roles in the human perception of pain (9,10) as they respond differently to noxious and innocuous stimuli of different modalities (11), communicate differently with different brain areas (9,12), and appear to receive a differential input from the two primary afferent nociceptor classes (5,13,14).

Relevant to the current study, we showed recently that extracranial injections of onabotulinumtoxinA inhibit responses of unmyelinated C-fibers to stimulation of their intracranial dural receptive fields with TRPV1 and TRPA1 agonists (15), as well as their responses to cortical spreading depression (CSD) (16), and that direct administration of onabotulinumtoxinA to the dural receptive fields of these nociceptors attenuated their mechanical sensitivity and prevented their sensitization by inflammatory mediators (17). However, the same extracranial injections of onabotulinumtoxinA did not prevent the activation of thinly myelinated Aδ-fibers to stimulation of their intracranial dural receptive fields with TRPV1/TRPA1 agonists (15) or their prolonged activation by CSD (16), and direct administration of onabotulinumtoxinA to their dural receptive field did not attenuate their responses to suprathreshold mechanical stimulation or their sensitization by inflammatory mediators (17). In contrast, we found that intravenous (IV) administration of the humanized monoclonal anti-calcitonin gene–receptor peptide (anti-CGRP) antibody (CGRP-mAb) fremanezumab inhibits responses to CSD in thinly myelinated Aδ- but not unmyelinated C-fibers (18), as well as responsiveness of HT but not WDR trigeminovascular neurons in the spinal trigeminal nucleus (STN) to mechanical stimulation of their dural receptive fields or their activation and sensitization by CSD (19).

While the mechanisms of action of these two classes of migraine preventive treatments differ greatly – onabotulinumtoxinA inhibits synaptic release of neurotransmitters or neuropeptides and insertion of new receptors to the presynaptic membrane (20,21) whereas fremanezumab neutralizes/inhibits CGRP – multiple randomized controlled trials showed that each reduces the number of migraine days per month significantly more than placebo (22,23). For most patients with chronic migraine, however, each of these drugs provides only partial relief. This knowledge has triggered an interest in determining whether a combination of such drugs may be more beneficial than the traditional monotherapy.

Theoretically, the ability of onabotulinumtoxinA to inhibit meningeal C- but not Aδ-fibers and that of fremanezumab to inhibit Aδ- but not C-fibers may explain some of the observed clinical benefits of such drugs for treatment of patients with chronic migraine (24). Since the perception of headache depends heavily on activation/sensitization of central trigeminovascular pathways, in this study we aimed to determine the effects of co-administration of onabotulinumtoxinA and atogepant on the two nociceptive classes of trigeminovascular neurons in the STN.

Methods

Experiments were approved by the Beth Israel Deaconess Medical Center and Harvard Medical School standing committees on animal care and were in accordance with the US National Institutes of Health's *Guide for the care and use of laboratory animals*. A total of 60 male Sprague-Dawley rats (240–300 g) were used. Of these, 20 rats were used to determine how best to administer atogepant, at what time to induce the CSD based on the drug's T_{max} and C_{max}, and which paralytic agent to use. Once these were determined, 40 consecutive rats were used and each yielded complete data for one neuron.

Overview of experimental protocol

An experimental protocol was designed to test the effect of combination treatment of onabotulinumtoxinA and atogepant on the activity of central trigeminovascular neurons in the dorsal horn (spontaneous activity and activity in response to peripheral stimulation and CSD) (Figure 1). Based on the time course of action of the two drugs, the onabotulinumtoxinA was administered 7 days prior to the day of neuronal recording, while atogepant was administered during the neuronal recording

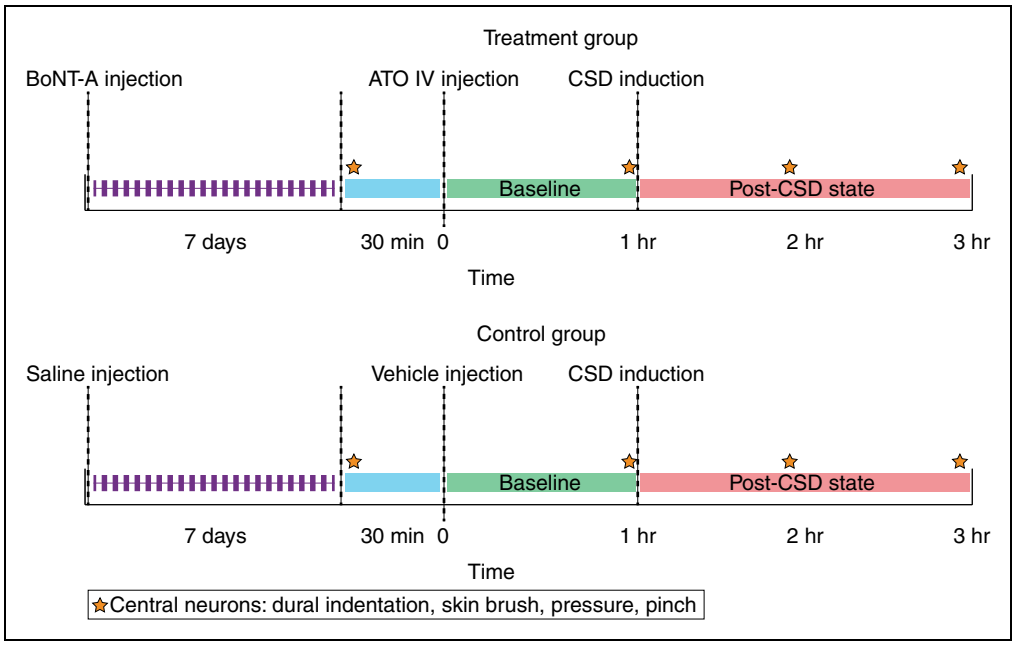

Figure 1. Experimental design. Treatment group received onabotulinumtoxinA injections to the scalp and intravenous atogepant. Control group received saline injections to the scalp and intravenous infusion of vehicle (50% dextrose water, 40% PEG 400, and 10% tocopherol). The star indicates the time at which responses to mechanical stimulation of the dura and skin were measured.
ATO: atogepant; BoNT-A: onabotulinumtoxinA; CSD: cortical spreading depression; IV: intravenous; PEG: polyethylene glycol.

session, 1 h prior to the induction of CSD. Two groups of rats were studied with this protocol: i) onabotulinumtoxinA-atogepant and ii) vehicle-vehicle. In this protocol, single-unit recordings of activity of central trigeminovascular neurons were obtained in anesthetized rats 7 days after scalp injection of onabotulinumtoxinA or vehicle. Thirty minutes after characterization of responses to dural and facial stimulation, rats received an IV infusion of atogepant or vehicle and their spontaneous activity (SA) was recorded for 1 h (this period is defined as the post-treatment/pre-CSD baseline). CSD was then induced and recording of neuronal activity continued for two more hours. Characterization of responses to dural and facial stimulation was repeated three times after the initial characterization: Immediately prior to CSD induction, and 1 h and 2 h after CSD induction (Figure 1). Ongoing discharge was recorded continuously throughout the experiment. Methodological details are described below.

Surgical preparation

Seven days after onabotulinumtoxinA or saline injection, rats were anesthetized with intraperitoneal urethane (0.9–1.2 g/kg) and surgically prepared for recording of neuronal activity in the STN as described in detail previously (11,19). The rats were intubated to allow artificial ventilation, and the femoral vein was cannulated for drug infusion. Core temperature and end-tidal CO_2 were monitored and kept within physiological range. Rats were paralyzed with rocuronium and ventilated. Data were used only in cases in which the physiological condition of the rats (heart rate, blood pressure, respiration, end-tidal CO_2) and the neuronal isolation signal (signal-to-noise ratio ~1:3) were stable throughout the experimental period. A craniotomy was made to expose the left transverse sinus, and a second craniotomy was made in the left parietal bone to allow recording of electrocorticogram activity and induction of CSD by pinprick. A segment of the spinal cord between the obex and C2 was exposed for recording of activity from central neurons in the left STN (C1-2 dorsal horn).

Identification and characterization of central trigeminovascular neurons

To record neuronal activity, a tungsten microelectrode (impedance 1–4 MΩ, FHC Co.) was lowered repeatedly into the STN (C1-2 dorsal horn) in search of central trigeminovascular neurons receiving input from the dura. Trigeminovascular neurons were first identified based on their responses to electrical stimulation of the dura. They were selected for the study if they exhibited discrete firing bouts in response to ipsilateral electrical (0.1–3.0 mA, 0.5 ms, 0.5 Hz pulses) and

mechanical (with calibrated von Frey monofilaments) stimulation of the exposed cranial dura.

Dural receptive fields were mapped by indenting the dura (4.19 g von Frey hair (VF) monofilament). Cutaneous receptive fields were mapped by applying innocuous and noxious mechanical stimulation to all facial skin areas as described previously (11). Responses to mechanical stimulation of the skin were determined by applying brief (10 sec) innocuous and noxious stimuli to the most sensitive portion of the cutaneous receptive field. Innocuous stimuli consisted of slowly passing a soft bristled brush across the cutaneous receptive field and pressure applied with a loose arterial clip. Noxious stimuli consisted of pinch with a strong arterial clip (11). Two classes of neurons were thus identified: WDR neurons (incrementally responsive to brush, pressure, and pinch) and HT neurons (unresponsive to brush). A real-time waveform discriminator was used to create and store a template for the action potential evoked in the neuron under study by electrical pulses on the dura; spikes of activity matching the template waveform were acquired and analyzed online and offline using Spike 2 software (Cambridge Electronic Design Limited).

At the conclusion of all experiments, a small electrolytic lesion was produced at the recording site, and its localization in the dorsal horn was determined post-mortem using histological analysis as described previously (25). Only one neuron was studied in each animal.

Treatment with onabotulinumtoxin-A

Seven days prior to surgical preparation, male Sprague Dawley rats (250–300 g) were briefly anesthetized (2% isoflurane) and injected with onabotulinumtoxinA (final dose = 5 U) or vehicle (normal saline). Four injections of onabotulinumtoxinA (each containing 1.25 U diluted in 5 μL saline) or saline (5 μL) were made along the lambdoid (two injection sites) and sagittal (two injection sites) sutures as described before (15).

Atogepant infusion

One hour prior to induction of CSD, atogepant or vehicle (50% dextrose water, 40% PEG 400, and 10% tocopherol) were administered intravenously at the same volume and rate. The final dose of atogepant was 5 mg/kg (5 mg/mL, 1 mL/kg, total infusion volume 0.24–0.3 mL, infusion rate 6 mL/min, ~30 sec total). To determine how much time should elapse before testing the effects of atogepant on CSD-induced activation, we first measured plasma concentration in three rats in which 5 mg/kg atogepant had been given intravenously and found that it was higher at 1 hour (2.0 μM) than at 2, 3, and 4 h after infusion (1.47, 1.29, and 1.11 μM, respectively).

CSD induction and electrocorticogram recording

One hour after atogepant infusion, CSD was induced as described before (19). For verification of CSD, electrocorticogram activity was recorded with a glass micropipette (0.9% saline, ~1 MΩ, 7 μm tip) placed just below the surface of the parietal cortex (~100 μm). We opted to use a single wave of CSD because patients rarely describe/experience more than one wave of aura in a single migraine attack; thus, this paradigm adheres better to the clinical reality (26,27).

Data analysis

Analyses of neuronal firing before and after induction of CSD and in responses to mechanical stimulation of the dura and skin, as well as their classification, was done by an experimenter who was blinded to the treatment each rat received (i.e. treatment with onabotulinumtoxinA/atogepant or with vehicle/saline). Randomization was applied to recording order of neuronal class (WDR and HT) and treatment (control, onabotulinumtoxinA/atogepant). To calculate the response magnitude to each stimulus (von Frey hairs [VFH] and mechanical stimulation of the skin), we subtracted the mean firing frequency occurring before the onset of the first stimulus (30 min for spontaneous activity, 10 sec for mechanical stimulation of the dura or skin) from the mean firing frequency that occurred throughout the duration of each stimulus; it was considered increased only if it reached more than 33% of their baseline response. To determine neuronal responses to CSD, the mean firing frequency occurring before the onset of CSD (calculated from measuring the SA during the 1 h period before CSD onset) was compared to the mean firing frequency recorded for 1 h (0–60 min after CSD) and 2 h (recorded from 60–120 min after CSD) after CSD induction. A neuron was considered activated if its mean firing rate after CSD exceeded its mean baseline activity by 1 SD for a period >10 min, which translated to an approximately > 33% increase in activity. To calculate the response to mechanical stimulation of the dura (VFH) and skin (brush, pressure, pinch), the mean firing frequency occurring before the onset of the first stimulus (mean spontaneous activity for 30 min) was subtracted from the mean firing frequency that occurred throughout the duration of each stimulus. Mean firing rates of respective values were compared using non-parametric repeated measures test (Friedman test) and *post-hoc* analysis (Tukey HSD – honestly significant difference). The level of significance was set at 0.05. To examine the

total proportion of responding HT and WDR neurons across the testing conditions, a generalized linear mixed model with a binomial distribution and log link was used to regress response onto treatment (control vs. treatment), test (spontaneous activity, VFH, brush, pressure, pinch), and treatment-by-test interaction. To accommodate repeated measurements, a random intercept was specified at the level of the neuron (i.e. each neuron received its own intercept) but dropped if a lack of neuron-level variance was observed.

Results

Baseline activity

The median (interquartile range, IQR) firing rates at baseline, prior to CSD induction, were 2.5 spikes/sec (0–9.6) for HT neurons in the control group, 1.7 spikes/sec (0–11.3) for HT neurons in the treatment group, 1.8 spikes/sec (0–5.1) for WDR neurons in the control group, and 2.5 spikes/sec (0–5.5) for WDR neurons in the treatment group. As noted below, there was no significant difference in baseline firing between neurons from animals treated with onabotulinumtoxinA and atogepant and neurons from animals treated with saline and vehicle ($p = 0.88$ [$Z = 0.14$, $n_1 = 10$, $n_2 = 10$], $p = 0.67$ [$Z = 0.42$, $n_1 = 10$, $n_2 = 10$], HT and WDR respectively, Wilcoxon signed-rank test).

When analyzing both types of neurons (HT and WDR) combined, the baseline median (IQR) rate prior to CSD induction was 2.5 spikes/sec (0–5.3) for all neurons in the control group and 1.7 spikes/sec (0–6.3) for all neurons in the treatment group. There was no significant difference in baseline firing between neurons from the control group and neurons from the treatment group ($p = 0.84$ [$Z = 0.19$, $n_1 = 20$, $n_2 = 20$], Wilcoxon signed rank test].

High-threshold neurons

CSD effects were tested on 20 HT neurons (control group, $n = 10$; treatment group, $n = 10$) in the deep laminae of the STN (Figure 2(a)–(b)). Their receptive fields included the intracranial dura (Figure 2(c)–(d)) and periorbital skin (Figure 2(e)–(f)). Typical CSD effects on spontaneous firing and responses to mechanical stimulation of the dura and skin are shown in Figure 3, where activation and sensitization occur in control (Figure 3(a)) but not treated (Figure 3(b)) animals.

Activation by CSD. In the control group, CSD triggered distinct and prolonged activation in 8/10 (80%) neurons, whereas in the treatment group, CSD activated only 1/10 (10%) neurons ($p = 0.001$, $\chi^2 = 9.8$, $DF = 1$, chi square) (Figure 4(a)). Firing rate analyses of all HT neurons (activated and non-activated) showed that, in the control group, baseline spontaneous activity (2.5 spikes/sec [0–9.6] (median, IQR)) increased significantly by 3.7 spikes/sec (0.45–7.2) (median, IQR) 1 h after CSD and by 5.3 spikes/sec (0.34–14.6) (median, IQR) 2 h after CSD ($\chi^2 = 6.4$, $DF = 2$, $p = 0.039$, Friedman test). *Post-hoc* (Tukey HSD) comparisons between baseline and 1 and 2 h post CSD onset yielded *p*-values of 0.021 and 0.014, respectively (Figure 5(a)). In contrast, in the treatment group, spontaneous activity remained unchanged after CSD. The neurons' baseline firing rate (1.7 spikes/sec [0–11.3] (median, IQR)) did not change significantly at 1 h (decrease of 0.2 spikes/sec [−0.9–0] (median, IQR) or 2 h (0 spikes/sec) [−1.9–0.7] (median, IQR) after CSD ($\chi^2 = 1.4$, $DF = 2$, $p = 0.35$, Friedman test) (Figure 5(b)).

Responses to mechanical stimulation of the dura. In the control group, baseline responses to dural indentation with calibrated VFH monofilament (4.1 g) (10.5 spikes/sec [4.7–33.3] (median, IQR)) increased by 6.7 spikes/sec (−0.8–15.5) (median, IQR) 1 h after CSD; and significantly increased by 10.1 spikes/sec (5.1–17.4) (median, IQR) 2 h after CSD ($\chi^2 = 6.4$, $DF = 2$, $p = 0.039$, Friedman test). *Post-hoc* (Tukey HSD) comparisons between baseline and 1 and 2 h post CSD onset yielded *p*-values of 0.056 and 0.049, respectively (Figure 6(a)). In the treatment group, baseline responses to dural indentation with the same VFH monofilament (5.2 spikes/sec [1.5–20.1] (median, IQR)) remained unchanged after CSD (decreased by 0.25 spikes/sec [−2.6–9] (median, IQR)) 1 h after CSD; and increased by 1 spike/sec (−2.4–6.8) (median, IQR) 2 h after CSD ($\chi^2 = 0.15$, $DF = 2$, $p = 0.97$, Friedman test)] (Figure 6(b)).

Responses to brush. In the control group, baseline responses to innocuous stimulation of the periorbital skin with a soft brush (0 spikes/sec [0 − 0] median, IQR) did not increase significantly after CSD (increased by 0.5 spikes/sec [0 − 22.6] (median, IQR)) 1 h after CSD; and by 9.6 spikes/sec (0 − 30.4) (median, IQR) 2 h after CSD ($\chi^2 = 3.75$, $DF = 2$, $p = 0.15$, Friedman test)] (Figure 7-I(a)). In the treatment group, skin brushing did not generate any activity before or after CSD (0 spikes/sec [0 − 0] (median, IQR)) before CSD; 0 spikes/sec (0 − 0) (median, IQR) 1 h after CSD; and 0 spikes/sec (0 − 0) (median, IQR) 2 h after CSD ($\chi^2 = 0$, $DF = 2$, $p = 1$, Friedman test)] (Figure 7-I(b)).

Responses to pressure. In the control group, baseline responses to application of pressure to the periorbital skin (8.4 spikes/sec [0 − 31.4] (median, IQR)) did not

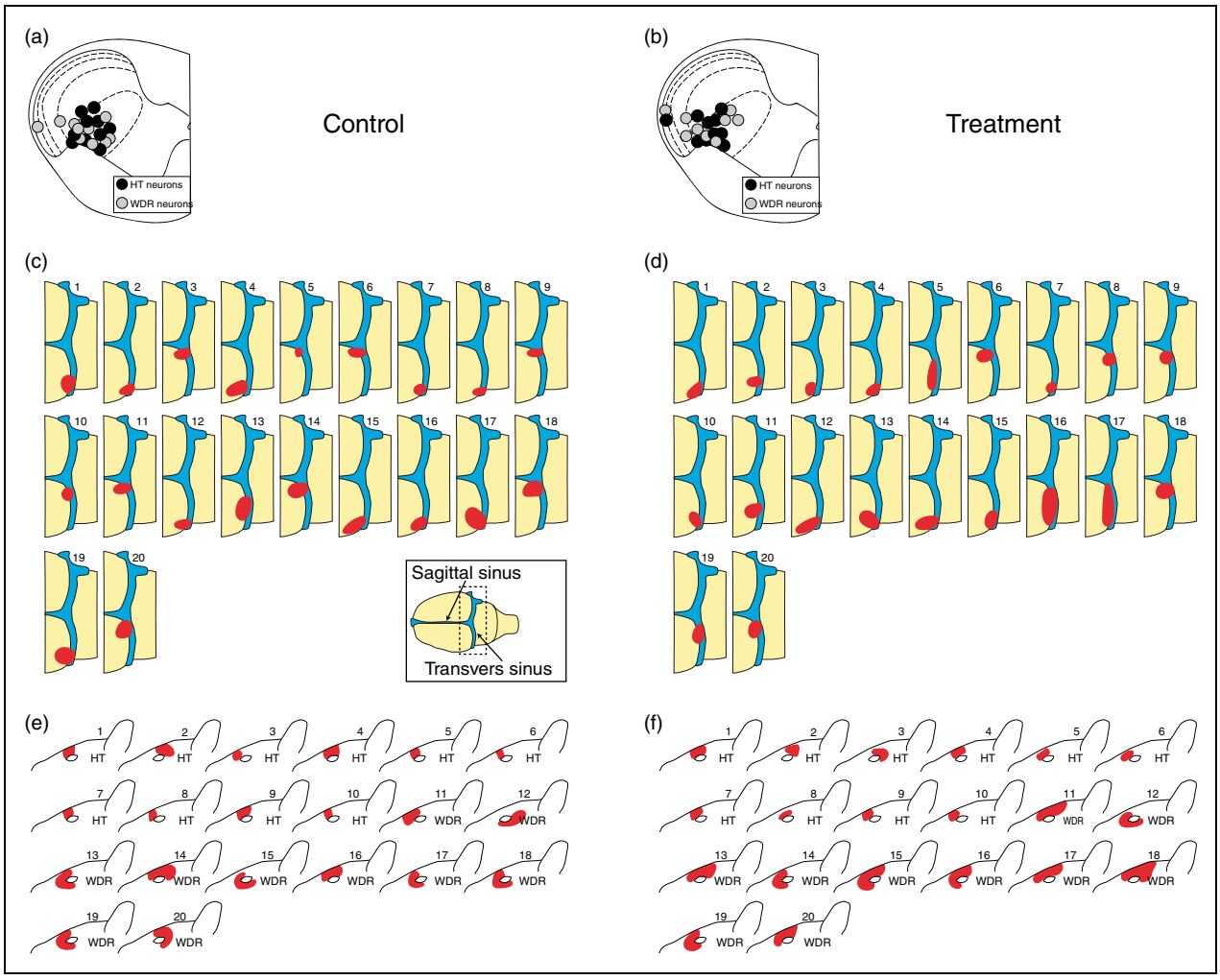

Figure 2. Recording sites ((a),(b)) and dural ((c),(d)) and facial ((e),(f)) receptive fields of all studied HT and WDR trigeminovascular neurons. Black and gray circles depict locations of lesions of HT and WDR neurons in the different laminae of the upper cervical spinal cord segment. Red indicates locations and sizes of most sensitive areas of dural and cutaneous receptive fields. Inset in (c) depicts dural receptive field drawings.
HT: high threshold; WDR: wide-dynamic range.

increase significantly after CSD (increased by 7.85 spikes/sec [−0.47–19.3] (median, IQR)) 1 h after CSD; and by 14 spikes/sec (−3.3–24.7) (median, IQR) 2 h after CSD ($\chi^2 = 2.6$, DF = 2, $p = 0.29$, Friedman test)] (Figure 7-II(a)). In the treatment group, responses to application of pressure to the skin (6.2 spikes/sec [2.7–25.6] (median, IQR)) also did not increase significantly after CSD (increased by 4.4 spikes/sec [−1.1–10.3] (median, IQR)) 1 h after CSD, and by 8.3 spikes/sec (−0.47–11.5) (median, IQR) 2 h after CSD ($\chi^2 = 3.35$, DF = 2, $p = 0.19$, Friedman test)] (Figure 7-II(b)).

Responses to pinch. In the control group, baseline responses to noxious stimulation of the skin with pinch (25.6 spikes/sec [11.9–37.6] (median, IQR)) did not increase significantly after CSD (increased by 7.3 spikes/sec [1.0–33.6] (median, IQR)) 1 h after CSD, and by 14.7 spikes/sec (−0.95–34.64) (median, IQR) 2 h after CSD ($\chi^2 = 5.6$, DF = 2, $p = 0.065$, Friedman test) (Figure 7-III(a)). In the treatment group, baseline responses to application of pressure to the skin (16.9 spikes/sec [7.5–34.9] (median, IQR)) also did not increase significantly after CSD (increased by 3.45 spikes/sec [−7.5–6.8] (median, IQR)) 1 h after CSD and by 9.2 spikes/sec (−5.35–21.02) (median, IQR) 2 h after CSD ($\chi^2 = 1.8$, DF = 2, $p = 0.43$, Friedman test) (Figure 7-III(b)).

Individual analysis. To better understand our findings, we also analyzed individual HT neurons' responses to dural and facial stimuli before and after CSD.

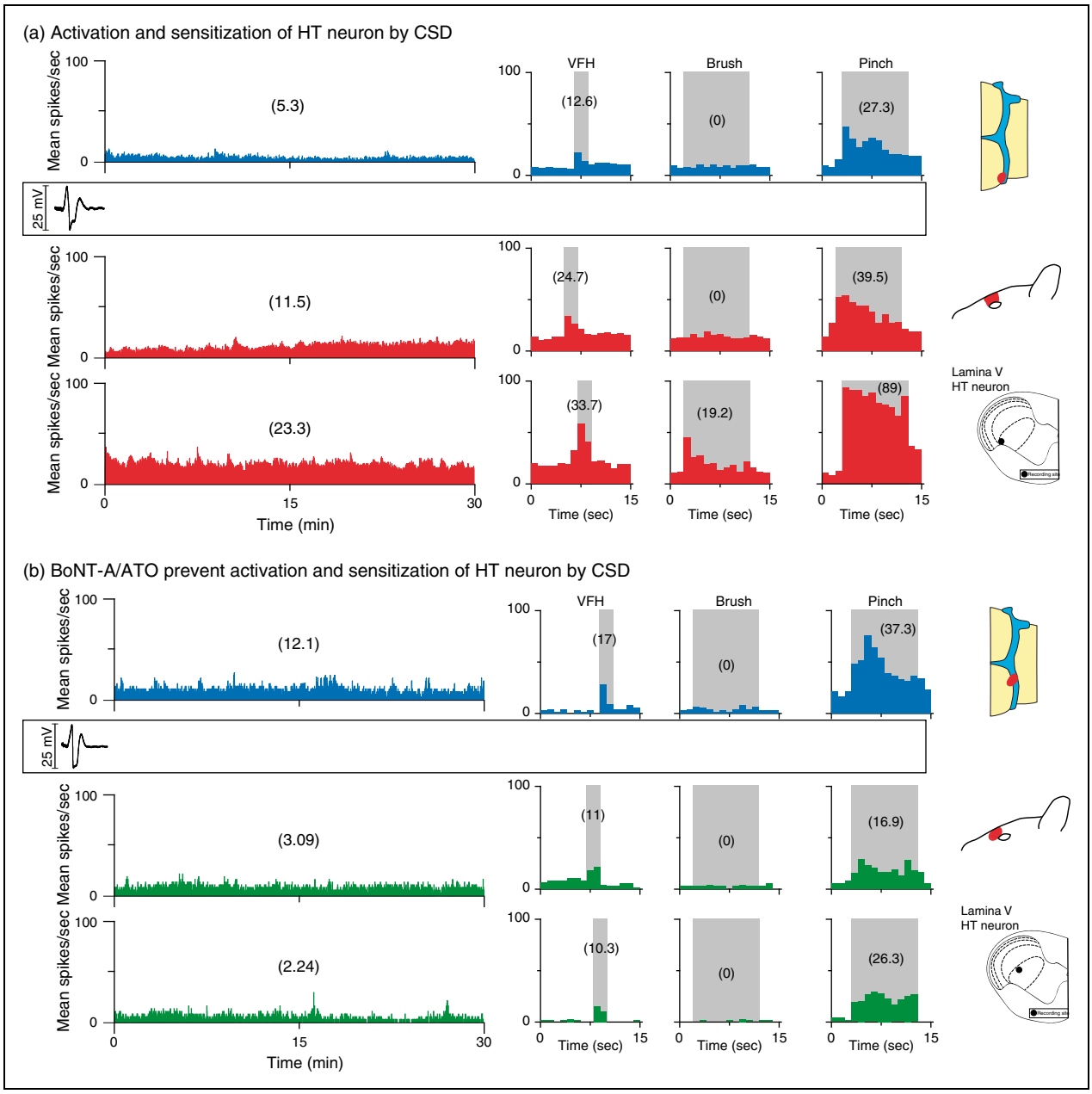

Figure 3. CSD effects on activation and sensitization of HT neurons in treated and untreated animals. (a) Plots of firing rate before (blue) and after (red) CSD induction in an animal treated with saline and vehicle (control). Note that spontaneous firing and responses to mechanical stimulation of the dura and skin increased after the CSD. (b) Plots of firing rate before (blue) and after (green) CSD induction in an animal treated with the combination of onabotulinumtoxinA and atogepant (treatment group). Note that spontaneous activity and responses to stimulation of the dura and skin did not increase after the CSD. Recording sites and locations of dural and cutaneous receptive fields are shown on the right.
CSD: cortical spreading depression; HT: high threshold; VFH: von Frey hair.

In the control group, the percentage of neurons that showed enhanced responses following CSD for these four stimuli were 80%, 60%, 80% and 80%, respectively. In contrast, in the treatment group, CSD induced enhanced firing in only 10%, 0%, 0%, and 0% of the HT neurons in response to VFH, brush, pressure, and pinch, respectively. Table 1 displays the aggregated responses across all testing conditions for both treatments. In the HT neurons, the treatment reduced the probability of response across all treatments (treatment main effect: $p = 0.002$). This effect did not differ across testing paradigms

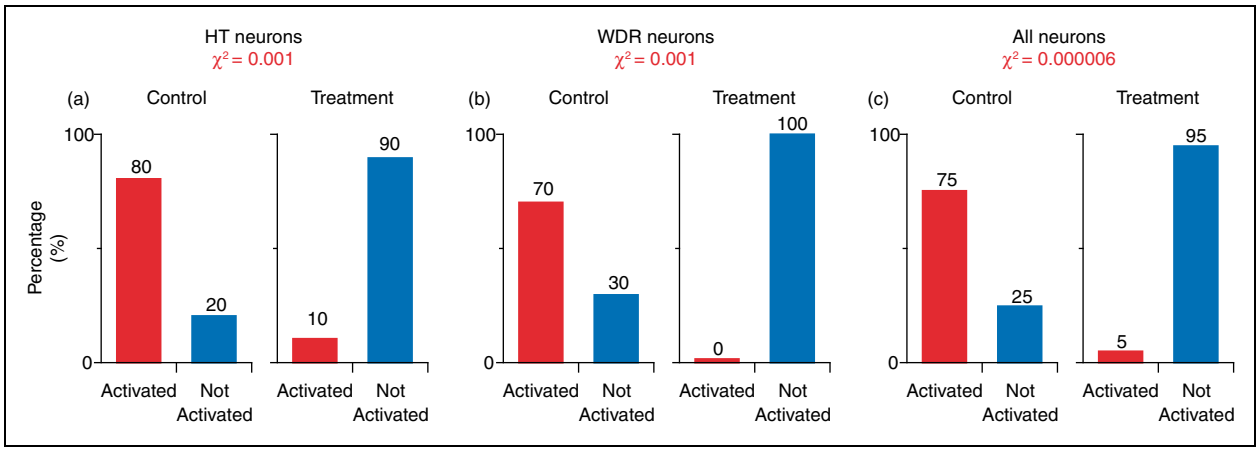

Figure 4. Percentage of neurons activated by CSD after combination treatment of onabotulinumtoxinA and atogepant (treatment group) or saline and vehicle (control) in HT (a), WDR (b) and all neurons (c). Chi square (χ^2) was used to calculate the level of significance of the percentage differences between the groups.
CSD: cortical spreading depression; HT: high threshold; WDR: wide-dynamic range.

(treatment × testing interaction: $p = 0.99$), indicating a consistent effect.

Wide-dynamic range neurons

CSD effects were tested on 20 WDR neurons (control group, n = 10, treatment group, n = 10) in the deep laminae of the STN (Figure 2(a)–(b)). Their receptive fields included the intracranial dura (Figure 2(c)–(d)) and periorbital skin (Figure 2(e)–(f)). Typical CSD effects on spontaneous firing and responses to mechanical stimulation of the dura and skin are shown in Figure 8, where activation and sensitization occurred in control (Figure 8(a)) but not treated (Figure 8(b)) animals.

Activation by CSD. In the control group, CSD triggered distinct and prolonged activation in 7/10 (70%) neurons, whereas, in the treatment group, CSD did not activate a single neuron (0%) ($p = 0.001$, $\chi^2 = 10.7$, DF = 1, chi square) (Figure 4(b)). Firing rate analyses of all WDR neurons (activated and non-activated) showed that, in the control group, baseline spontaneous activity (1.8 spikes/sec [0–5.1] (median, IQR)) increased significantly by 1.5 spikes/sec (0–11.8) (median, IQR) 1 h after CSD; and by 1.2 spikes/sec (0–2.9) (median, IQR) 2 h after CSD ($\chi^2 = 7.8$, DF = 2, $p = 0.004$, Friedman test). *Post-hoc* (Tukey HSD) comparisons between baseline and 1 and 2 h post CSD onset yielded *p*-values of 0.023 and 0.023, respectively (Figure 5(c)). In contrast, in the treatment group, despite the CSD, spontaneous activity showed a significant decrease rather than an increase (2.5 spikes/sec [0.07–5.5] (median, IQR)) before CSD; decreased by 0.9 spikes/sec (−3.4–0.07) (median, IQR) 1 h after CSD; and by 0.1 spikes/sec (−3–0.07) (median, IQR) 2 h after CSD ($\chi^2 = 8.6$, DF = 2, $p = 0.003$, Friedman test). *Post-hoc* (Tukey HSD) comparisons between baseline and 1 and 2 h post CSD onset yielded *p*-values of 0.01 and 0.23, respectively (Figure 5(d)).

Responses to mechanical stimulation of the dura. In the control group, baseline responses to dural indentation with calibrated VFH monofilament (4.1 g) (9.3 spikes/sec [5.8–19.4] (median, IQR)) did not increase significantly after CSD (increased by 4.1 spikes/sec [−0.8–15] (median, IQR) 1 h after CSD; and by 5.4 spikes/sec (0.6–12.1) (median, IQR) 2 h after CSD ($\chi^2 = 4.8$, DF = 2, $p = 0.089$, Friedman test)] (Figure 6(c)). In the treatment group, baseline responses to dural indentation with the same VFH monofilament (4.0 spikes/sec [1.3–9.8] (median, IQR)) decreased (rather than increased), though insignificantly, after CSD (decreased by 1.25 spikes/sec [−3.25–0.9] (median, IQR) 1 h after CSD; and increased by 0.25 spikes/sec (−3–1.75) (median, IQR) 2 h after CSD ($\chi^2 = 1.95$, DF = 2, $p = 0.35$, Friedman test).] (Figure 6(d)).

Responses to brush. In the control group, baseline responses to innocuous stimulation of the periorbital skin with a soft brush (13.5 spikes/sec [3.5–20.0] (median, IQR)) increased significantly after CSD (increased by 10.6 spikes/sec [0.9–16.5] (median, IQR)) 1 h after CSD; and by 7.6 spikes/sec (2.1–14.3) (median, IQR) 2 h after CSD ($\chi^2 = 8.5$, DF = 2, $p = 0.013$, Friedman test). *Post-hoc* (Tukey HSD) comparisons between baseline and 1 and 2 h post CSD onset yielded *p*-values of 0.013 and 0.011, respectively (Figure 7-I(c)). Unlike in the HT group, however, baseline responses to brushing of the skin (9.3 spikes/sec [5.1–14.9] (median, IQR)) increased significantly 2 h

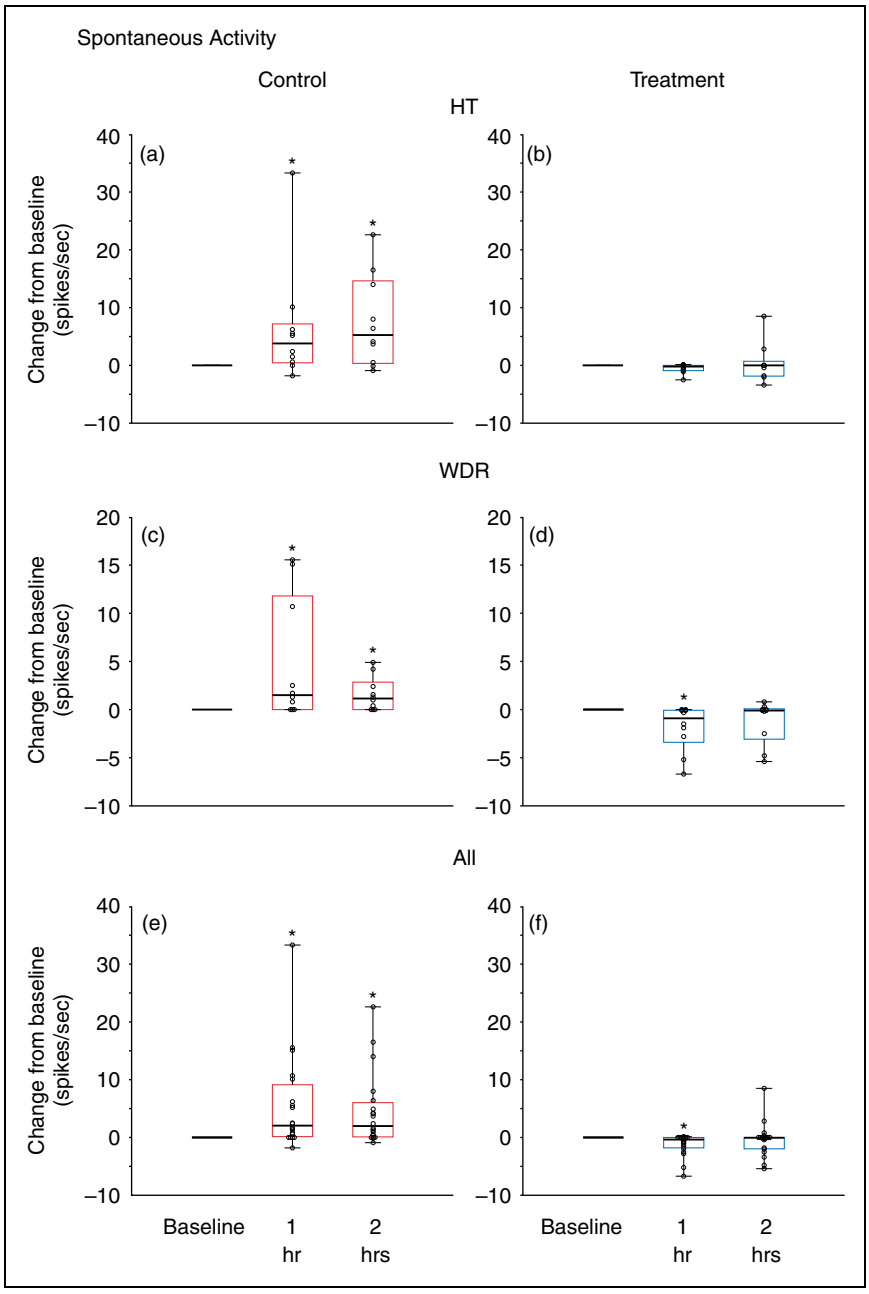

Figure 5. Changes from baseline in spontaneous activity at 1 and 2 h after CSD induction, shown in box-and-whisker plots combined with scatterplots of individual values, for control (in red; (a), (c), (e)) and treatment (in blue; (b), (d), (f)) groups. (a) and (b) HT neurons (n = 10 per group); (c) and (d) WDR neurons (n = 10 per group); (e) and (f) all neurons (n = 20 per group).
*$p < 0.05$ Friedman test; *post-hoc*/Tukey HSD.
CSD: cortical spreading depression; HT: high threshold; WDR: wide-dynamic range.

after the CSD, in spite of the treatment (increased by 1.2 spikes/sec [−1.6–10.9] (median, IQR)) 1 h after CSD; and by 7.3 spikes/sec (4.1 – 20.2) (median, IQR) 2 h after CSD ($\chi^2 = 7.8$, DF = 2, $p = 0.022$, Friedman test). *Post-hoc* (Tukey HSD) comparisons between baseline and 1 and 2 h post CSD onset yielded *p*-values of 0.23 and 0.0048, respectively (Figure 7-I(d)).

Responses to pressure. In the control group, baseline responses to application of pressure to the periorbital skin (22.8 spikes/sec [5.9 – 25.7] (median, IQR)) increased significantly after CSD (increased by 11.5 spikes/sec [2.42 – 19.8] (median, IQR)) 1 h after CSD; and by 11.1 spikes/sec (1.6 – 26.5) (median, IQR) 2 h after CSD ($\chi^2 = 9.05$, DF = 2, $p = 0.0106$, Friedman test)]. *Post-hoc* (Tukey HSD) comparisons between

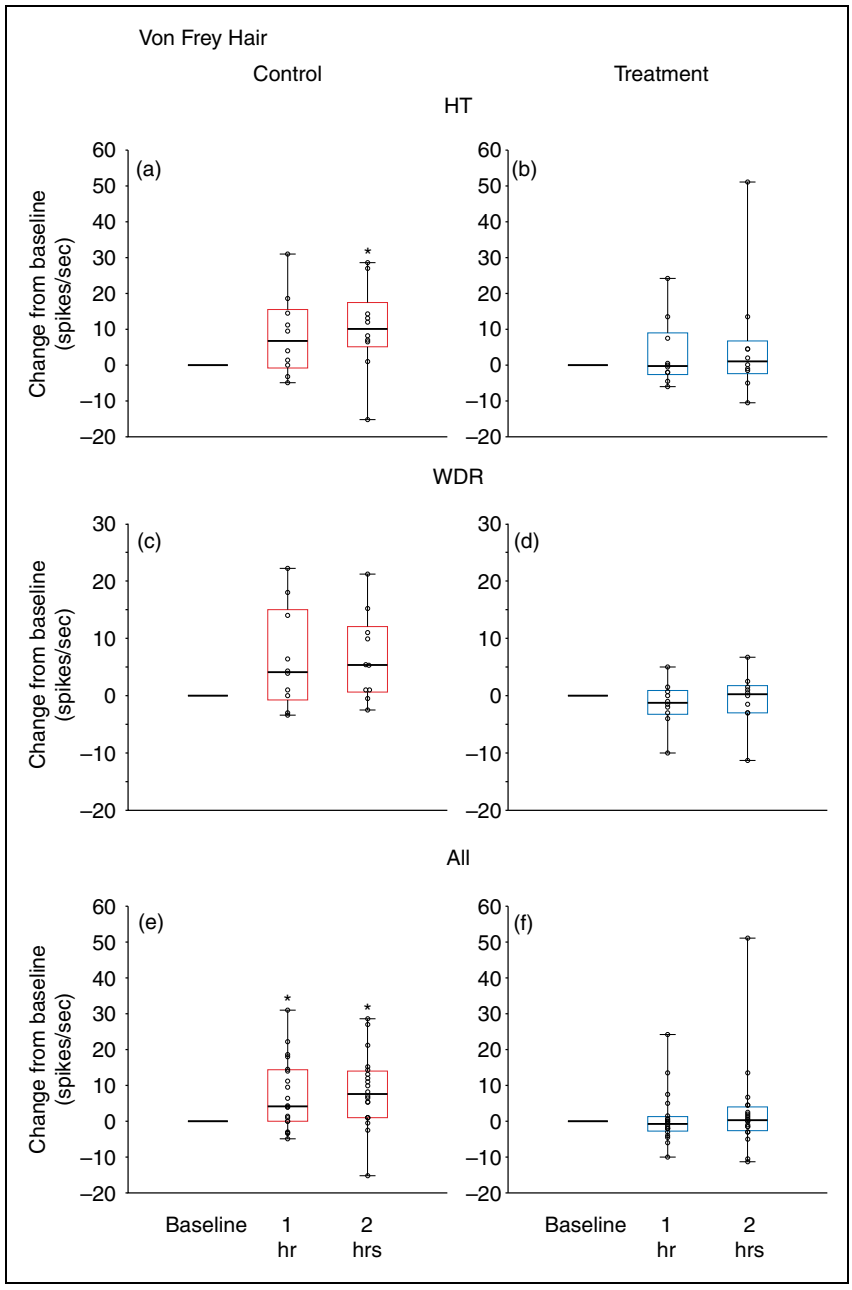

Figure 6. Changes from baseline in response to dural indentation at 1 and 2 h after CSD induction, shown in box-and-whisker plots combined with scatterplots of individual values, for control (in red; (a), (c), (e)) and treatment (in blue; (b), (d), (f)). (a) and (b) HT neurons (n = 10 per group); (c) and (d) WDR neurons (n = 10 per group); (e) and (f) all neurons (n = 20 per group).
*$p < 0.05$ Friedman test; *post-hoc*/Tukey HSD.
CSD: cortical spreading depression; HT: high threshold; WDR: wide-dynamic range.

baseline and 1 and 2 h post CSD onset yielded *p*-values of 0.014 and 0.0058, respectively (Figure 7-II(c)). In the treatment group, baseline responses to application of pressure to the skin (14.9 spikes/sec [8.9 – 17.3] (median, IQR)) remained unchanged after CSD (decreased by 2 spikes/sec [−3.7–26.82] (median, IQR)) 1 h after CSD; and increased by 16.0 spikes/sec (−1.5–23.2) (median, IQR)) 2 h after CSD [($\chi^2 = 3.2$, DF = 2, $p = 0.21$, Friedman test)] (Figure 7-II(d)).

Responses to pinch. Despite the CSD, responses to noxious stimulation of the skin with pinch remained unchanged in both the control and the treatment groups. Responses in the control group were 30 spikes/sec (8.6–43.9) (median, IQR) before CSD;

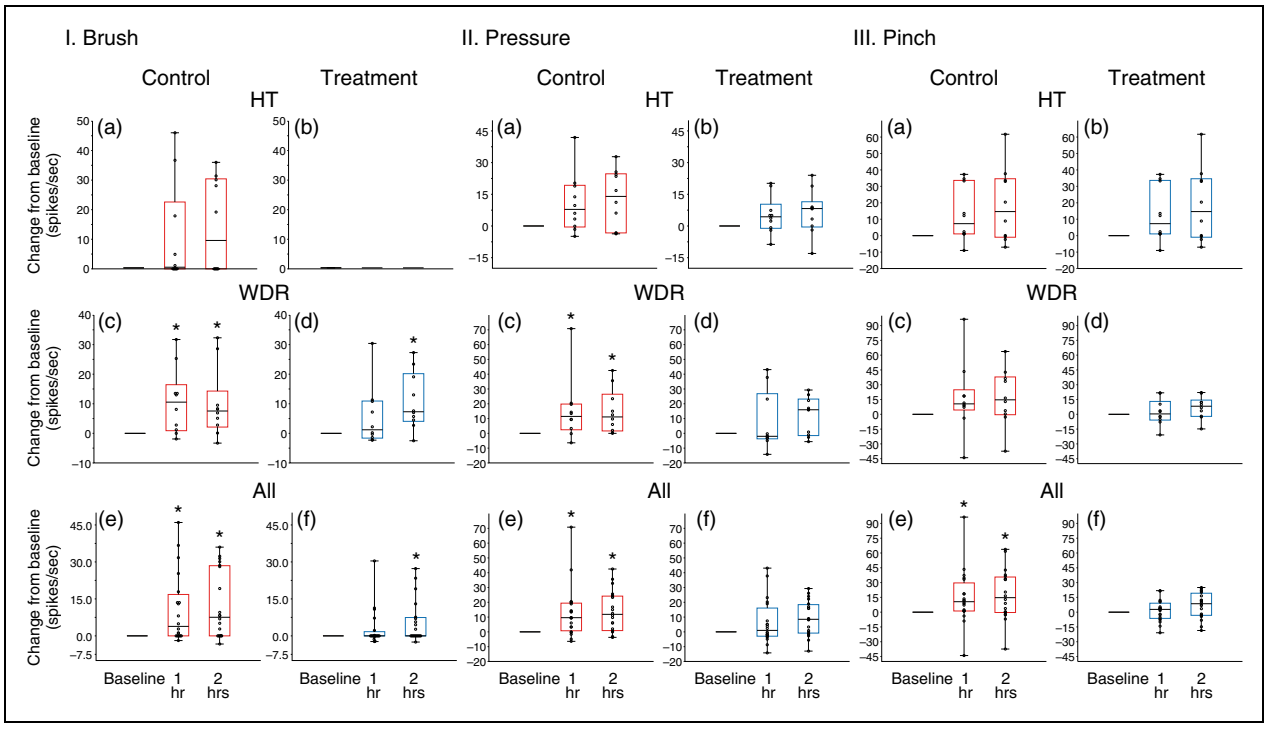

Figure 7. Changes from baseline in responses to mechanical stimulation of the skin (I. brush, II. pressure, and III. pinch) at 1 and 2 h after CSD induction, shown in box-and-whisker plots combined with scatterplots of individual values, for control (in red; (a),(c),(e)) and treatment (in blue; (b),(d),(f)). (a) and (b) HT neurons (n = 10 per group); (c) and (d) WDR neurons (n = 10 per group); (e) and (f) all neurons (n = 20 per group).
*$p < 0.05$ Friedman test; *post-hoc*/Tukey HSD.
CSD: cortical spreading depression; HT: high threshold; WDR: wide-dynamic range.

increased by 10.6 spikes/sec (4.4–24.9) (median, IQR) 1 h after CSD; and by 14.7 spikes/sec (−0.4–37.9) (median, IQR) 2 h after CSD ($\chi^2 = 5.4$, DF = 2, $p = 0.072$, Friedman test) (Figure 7-III(c)). Responses in the treatment group were 21.3 spikes/sec (12.9–29.9) (median, IQR) before CSD, increased by 0.4 spikes/sec (−5.9–13.1) (median, IQR) 1 h after CSD; and by 8.2 spikes/sec (−2.1–14.42) (median, IQR]) 2 h after CSD ($\chi^2 = 2.4$, DF = 2, $p = 0.32$, Friedman test) (Figure 7-III(d)).

Individual analysis. To better understand our findings, we also analyzed individual WDR neurons' responses to dural and facial stimuli before and after CSD. In the control group, 60%, 70%, 70%, and 60% exhibited enhanced firing in response to VFH, brush, pressure, and pinch, respectively. In contrast, in the treatment group, CSD induced enhanced firing in only 10%, 5%, 0%, and 0% of the WDR neurons in response to VFH, brush, pressure and pinch, respectively. Table 1 displays the aggregated responses across all testing conditions for both treatments. In the WDR neurons, the treatment reduced the probability of response across all treatments (treatment main effect: $p = 0.021$) with a treatment x testing interaction effect ($p = 0.025$) that was driven by development of brush sensitization in the treatment group.

All neurons

Activation by CSD. In the control group, CSD triggered distinct and prolonged activation in 75% of all studied neurons, whereas in the treatment group, CSD activated 5% of the neurons ($p = 0.000006$, $\chi^2 = 20.4$, DF = 1, chi square) (Figure 4(c)). Firing rate analyses of all neurons (activated and non-activated) showed that in the control group, baseline spontaneous activity (2.5 spikes/sec [0–5.3] (median, IQR)) increased significantly after CSD by 2.1 spikes/sec (0.2–9.1) (median, IQR) 1 h after CSD; and 2.0 spikes/sec (0.1–6.0) (median, IQR) 2 h after CSD ($\chi^2 = 13.7$, DF = 2, $p = 0.00029$, Friedman test). *Post-hoc* (Tukey HSD) comparisons between baseline and 1 and 2 h post CSD onset yielded *p*-values of 0.0004 and 0.0001, respectively (Figure 5 (e)). In contrast, in the treatment group, despite the CSD, spontaneous activity showed a significant decrease rather than an increase (1.7 spikes/sec [0–6.3] (median, IQR)) before CSD, decreased by 0.4 spikes/sec (−1.8–0) (median, IQR) 1 h after CSD; and 0.05 spikes/sec (−2.0–0) (median, IQR) 2 h after CSD

Table 1. Individual analysis of neuronal responses.

	Spontaneous activity	Von Frey hair (dura)	Brush	Pressure	Pinch
High threshold					
CTL					
Group analysis	Activation/sensitization	Sensitization	No sensitization	No sensitization	No sensitization
Individual analysis	Activated: 8/10	Sensitized: 8/10	Sensitized: 6/10	Sensitized: 8/10	Sensitized: 6/10
RX					
Group analysis	Prevention	Prevention	No sensitization	No sensitization	No sensitization
Individual analysis	Activated: 1/10	Sensitized: 1/10	Sensitized: 0/10	Sensitized: 0/10	Sensitized: 0/ 10
Wide-dynamic range					
CTL					
Group analysis	Activation/sensitization	No sensitization	Sensitization	Sensitization	No sensitization
Individual analysis	Activated: 7/10	Sensitized: 6/10	Sensitized: 7/10	Sensitized: 7/10	Sensitized: 7/10
RX					
Group analysis	Inhibition	No sensitization	Sensitization (2 hr)	Prevention	No sensitization
Individual analysis	Activated: 0/10	Sensitized: 0/ 10	Sensitized: 5/10	Sensitized: 0/10	Sensitized: 0/10:
All neurons					
CTL					
Group analysis	Activation/sensitization	Sensitization	Sensitization	Sensitization	Sensitization
Individual analysis	Activated: 15/20	Sensitized: 14/20	Sensitized: 13/20	Sensitized: 15/20	Sensitized: 13/20
RX					
Group analysis	Inhibition	Prevention	Prevention	Prevention	Prevention
Individual analysis	Activated: 1/20	Sensitized: 1/ 20	Sensitized: 5/20	Sensitized: 0/20	Sensitized: 0/20

($\chi^2 = 8.1$, DF = 2, p = 0.002, Friedman test). Post-hoc (Tukey HSD) comparisons between baseline and 1 and 2 h post CSD onset yielded p-values of 0.0006 and 0.26, respectively (Figure 5(f)).

Responses to mechanical stimulation of the dura. In the control group, baseline responses to dural indentation with calibrated VFH monofilament (4.1 g) (9.3 spikes/sec [5.6–23.7] (median, IQR) increased significantly after CSD by 4.2 spikes/sec (0–14.4) (median, IQR) 1 h after CSD; and by 7.6 spikes/sec (1–14) (median, IQR) 2 h after CSD ($\chi^2 = 11.2$, DF = 2, p = 0.0033, Friedman test). Post-hoc (Tukey HSD) comparisons between baseline and 1 and 2 h post CSD onset yielded p-values of 0.003 and 0.002, respectively (Figure 6(e)). In the treatment group, responses to dural indentation with the same VFH monofilament (4.7 spikes/sec [1.5–10.8] (median, IQR)) remained unchanged after CSD (reduced by 0.75 spikes/sec [−2.8–1.3] (median, IQR)) 1 h after CSD; and increased by 0.3 spikes/sec (−2.6–4) (median, IQR) 2 h after CSD ($\chi^2 = 3.9$, DF = 2, p = 0.14, Friedman test)] (Figure 6(f)).

Responses to brush. In the control group, baseline responses to innocuous stimulation of the periorbital skin with a soft brush (0.65 spikes/sec [0–14.1] (median, IQR)) did not increase significantly after CSD; increased by 3.9 spikes/sec (0–16.8) (median, IQR) 1 h after CSD; and increased by 7.55 spikes/sec (0–28.5) (median, IQR) 2 h after CSD ($\chi^2 = 4.2$, DF = 2, p = 0.10, Friedman test (Figure 7-I(e)). In contrast, in the treatment group, despite the CSD, baseline responses to brushing of the skin (0.4 spikes/sec [0–9.7] (median, IQR)) showed a significant decrease rather than an increase 2 h after the CSD; increased by 0 spikes/sec (0–1.7) (median, IQR) 1 h after CSD; and by 0 spikes/sec (0–7.5) (median, IQR) 2 h after CSD ($\chi^2 = 3.9$, DF = 2, p = 0.021, Friedman test). Post-hoc (Tukey HSD) comparisons between baseline and 1 and 2 h post CSD onset yielded p-values of 0.23 and 0.0048, respectively (Figure 7-I(f)).

Responses to pressure. In the control group, baseline responses to application of pressure to the periorbital skin (12.1 spikes/sec [5.4–25.1] (median, IQR)) increased significantly after CSD; increased by 10.6 spikes/sec (1.2–29.7) (median, IQR) 1 h after CSD; and by 14.7 spikes/sec (−0.4–35.7) (median, IQR) 2 h after CSD ($\chi^2 = 10.6$, DF = 2, p = 0.0046, Friedman test). *Post-hoc* (Tukey HSD) comparisons between baseline and 1 and 2 h post CSD onset yielded p-values of 0.0015 and 0.00026, respectively (Figure 7-II (e)). In the treatment group, baseline responses to application of pressure to the skin (13.9 spikes/sec [6.7–22.9] (median, IQR)) remained unchanged after CSD (increased by 2.8 spikes/sec [−6.3–9.1] (median, IQR) 1 h after CSD; and increased by 8.6 spikes/sec (−3.2–19.2) (median, IQR) 2 h after CSD ($\chi^2 = 4.2$, DF = 2, p = 0.11, Friedman test) (Figure 7-II(f)).

Responses to pinch. In the control group, baseline responses to noxious stimulation of the skin with

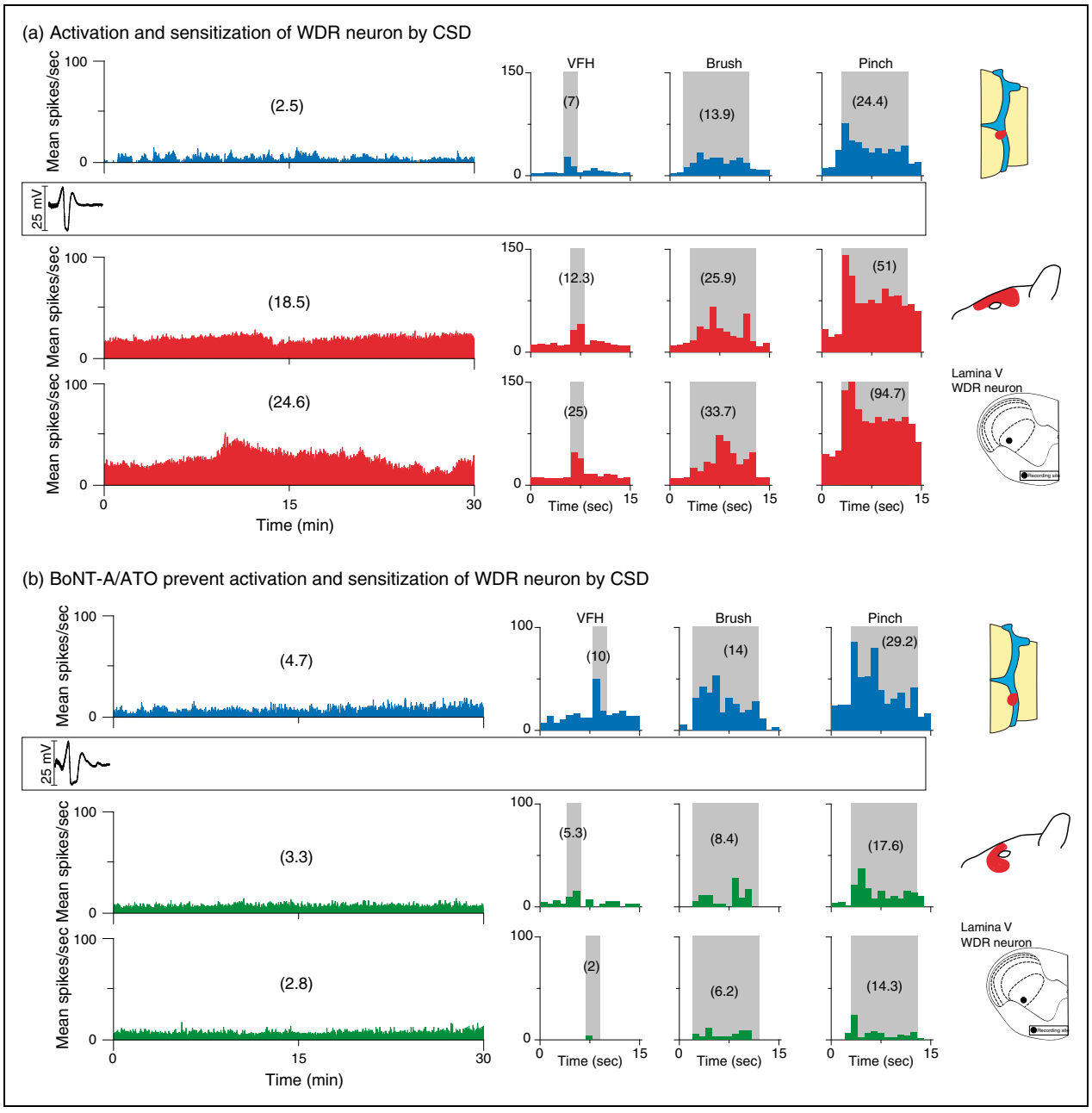

Figure 8. CSD effects on activation and sensitization of WDR neurons in treated and untreated animals. (a) Plots of firing rate before (blue) and after (red) CSD induction in an animal treated with saline and vehicle (control). Note that spontaneous firing and responses to mechanical stimulation of the dura and skin increased after the CSD. (b) Plots of firing rate before (blue) and after (green) CSD induction in an animal treated with the combination of onabotulinumtoxinA and atogepant (treatment group). Note that spontaneous activity and responses to stimulation of the dura and skin did not increase after the CSD. Recording sites and locations of dural and cutaneous receptive fields are shown on the right.
CSD: cortical spreading depression; WDR: wide-dynamic range.

pinch (28.1 spikes/sec [9.9–40.9] (median, IQR)) increased significantly after CSD ($\chi^2 = 10.9$, DF = 2, p = 0.0044, Friedman test). Responses increased by 40.6 spikes/sec (26.6–54.6) (median, IQR) 1 h after CSD, and by 40.3 spikes/sec (26.5–66.5) (median, IQR) 2 h after CSD. Post-hoc (Tukey HSD) comparisons between baseline and 1 and 2 h post CSD onset yielded p-values of 0.0064 and 0.0089, respectively (Figure 7-III(e)). In the treatment group, responses to pinching the skin remained unchanged after CSD (19.6 spikes/sec [12.1–33.6] (median, IQR)) before CSD; 16.4 spikes/sec (9.2–41.3) (median, IQR)

1 h after CSD; and 30.3 spikes/sec (13.2–41.5) (median, IQR) 2 h after CSD ($\chi^2 = 3.9$, DF = 2, p = 0.14, Friedman test)] (Figure 7-III(d)).

Individual analysis. To better understand our findings, we also analyzed all individual neurons' responses to dural and facial stimuli before and after CSD. In the control group, 70%, 65%, 75%, and 65% exhibited enhanced firing in response to VFH, brush, pressure, and pinch, respectively. In contrast, in the treatment group, CSD induced enhanced firing in only 5%, 25%, 0%, and 0% of all the neurons in response to VFH, brush, pressure, and pinch, respectively (Table 1).

Discussion

Using single-unit recording techniques and an established animal model of migraine, we show that combined onabotulinumtoxinA/atogepant pre-treatment in rats prevents CSD-induced activation and sensitization of almost all nociceptive trigeminovascular neurons in the STN. Consistent with our hypothesis, the combination therapy was effective in inhibiting both the HT and the WDR neuron populations. We also show that pre-treatment with scalp injections of saline and IV injections of vehicle do not prevent the prolonged activation and sensitization of both HT and WDR neurons by a single wave of CSD, induced by a pinprick. While these conclusions are generally true for both HT and WDR neurons, it appears that the effects of this combination treatment are more pronounced in the WDR neurons. Given the preferential inhibitory effects of onabotulinumtoxinA on unmyelinated C- but not thinly myelinated Aδ-fibers (15–17), and the preferential inhibitory effects of fremanezumab on Aδ- but not C-fibers (18) and on HT but not WDR neurons (19), it is reasonable to propose that the robust inhibition of activation and sensitization of the trigeminovascular HT and WDR neurons by the onabotulinumtoxinA/atogepant treatment was achieved through a dual blockade of both classes of meningeal nociceptors. These findings emphasize the need to determine drug effects on all classes of peripheral and central trigeminovascular neurons, and call attention to the possibility that a combination therapy that inhibits meningeal C-fibers and directly or indirectly prevents CGRP from activating its receptors on Aδ-meningeal nociceptors (by inhibiting CGRP signalling in the meninges) may be more effective than a monotherapy in reducing migraine days per month in those with chronic migraine, a view partially supported by a recent open-label study (24).

Clinically, the use of combination drug therapy has a strong rationale that is based on growing understanding of the multiple mechanisms involved in the generation of pain and headache. The background for choosing to combine onabotulinumtoxinA and atogepant is summarized below. Briefly, onabotulinumtoxinA is a chronic migraine preventive treatment that significantly reduces headache frequency (22,28). It is thought to achieve its anti-migraine effects by inhibiting exocytosis of neuropeptides/neurotransmitters from cranial and pericranial sensory and motor nerve endings, and by blocking the insertion of new receptor protein into the membrane – all through its ability to enter neurons (29,30), cleave SNAP-25 (29), and inhibit SNARE-mediated vesicle trafficking (31). We chose it for its repeatedly demonstrated ability to selectively inhibit C- but not Aδ-meningeal nociceptor responses to activation and sensitization by inflammatory mediators (17), TRPV1 and TRPA1 agonists (15), and CSD (16). In contrast, atogepant is a small molecule CGRP receptor antagonist (CGRP-RA) that blocks CGRP signalling by binding to CLR+RAMP1 CGRP receptors and CTR+RAMP1 amylin receptors outside the central nervous system (32,33). It is one of several small molecule CGRP-RAs developed recently for acute (rimegepant, ubrogepant) and preventive (rimegepant, atogepant) treatment of migraine (34–37). While the way by which atogepant blocks CGRP signalling differs from the way anti-CGRP monoclonal antibodies such as fremanezumab, eptinezumab, and galcanezumab block CGRP signalling (the latter by neutralizing the CGRP molecule), the two classes of drugs are believed to achieve their therapeutic effects by preventing activation of intracranial CGRP receptors in sensory neurons (38) and the vasculature (39). We chose atogepant over a CGRP-mAb because it differs enough in its mechanism of action (e.g. monoclonal antibody targeting the peptide vs. antagonist targeting the receptor, small vs. larger molecule, daily oral pill vs. monthly injection) to allow us to determine whether it is a drug-specific effect or a class-specific effect (i.e. all drugs capable of inhibiting CGRP signalling in the meninges). Relevant to their mechanisms of action in the prevention/termination of the headache phase of migraine are two sets of data showing that CGRP receptors are found in Aδ- but not in C-fiber meningeal nociceptors (38), and that CSD-induced activation and sensitization of Aδ- but not C-fibers (18) and consequently HT but not WDR neurons (19) are prevented by the CGRP-mAb fremanezumab. An additional study using the CGRP antagonist BIBN4096 reported that the incidence of CSD-induced activation in meningeal Aδ fibers was 47% in animals that received dimethyl sulfoxide and 31% when BIBN4096 was administered (40).

Until very recently, no drug tested in animal models of migraine or in physiological studies of peripheral and central trigeminovascular neurons looked at or

found selectivity to any one class of peripheral (C-, Aδ-) or central (HT, WDR) trigeminovascular neurons. However, recent studies showing respective blockade of meningeal C- and Aδ-fiber activation by onabotulinumtoxinA and fremanezumab (15–19) call attention to the possibility that partial relief or prevention of the headache phase of migraine by some of the most common migraine abortive and prophylactic drugs may be explained by their inability to block all classes of meningeal nociceptors, thus allowing some pain signals to reach the STN.

In summary, the current study provides scientific rationale for carrying out controlled clinical studies to test the possibility that a combination therapy that targets activation of meningeal C- and Aδ-fibers with onabotulinumtoxinA and any one of the drugs that prevent activation of CGRP receptors on the Aδ-fibers is more effective than a monotherapy. This approach is based on two assumptions, which have not been confirmed. The first is that by blocking CGRP signalling in the meninges, the small molecule CGRP-RA atogepant inhibits responses to CSD in Aδ meningeal nociceptors and, consequently, HT trigeminovascular neurons in the STN similarly to the CGRP monoclonal antibody fremanezumab. The second is that by inhibiting meningeal C-fiber responses to CSD, onabotulinumtoxinA also attenuates activation of central trigeminovascular WDR neurons. Finally, we must remember that these electrophysiological studies were carried out in anesthetized rats rather than awake patients with migraine and, as such, should serve as rationale/justification for designing clinical studies.

Key findings

- CSD-induced activation and sensitization of nearly all trigeminovascular HT and WDR neurons in the spinal trigeminal nucleus are blocked by simultaneous administration of onabotulinumtoxinA and atogepant – likely through attenuation of C- and Aδ-meningeal nociceptors.
- The results highlight the importance of distinguishing between drugs that inhibit Aδ fibers only, C-fibers only, HT neurons only, WDR neurons and any combination of the above as it may improve the reliability of preclinical models of migraine.
- The results provide a preclinical rationale for clinical studies that evaluate whether the risk/benefit ratio of this combination therapy is superior to the risk/benefit ratio of a monotherapy in reducing migraine days per month in patients with chronic migraine.

Acknowledgements

The authors thank Brenda B Smith for assistance in analyzing the pharmacodynamics and pharmacokinetics of atogepant.

Declaration of conflicting interests

The authors declared no potential conflicts of interest with respect to the research, authorship, and/or publication of this article.

Funding

The authors disclosed receipt of the following financial support for the research, authorship, and/or publication of this article: This study was funded by a grant from Allergan (before its acquisition by AbbVie) and NIH grants NS079678, NS094198, NS106345 to RB and AMS.

References

1. Mayberg M, Langer RS, Zervas NT, et al. Perivascular meningeal projections from cat trigeminal ganglia: Possible pathway for vascular headaches in man. *Science* 1981; 213: 228–230.
2. Ashina M, Hansen JM, Do TP, et al. Migraine and the trigeminovascular system – 40 years and counting. *Lancet Neurol* 2019; 18: 795–804.
3. May A and Goadsby PJ. The trigeminovascular system in humans: Pathophysiologic implications for primary headache syndromes of the neural influences on the cerebral circulation. *J Cereb Blood Flow Metab* 1999; 19: 115–127.
4. Burstein R, Noseda R and Borsook D. Migraine: Multiple processes, complex pathophysiology. *J Neurosci* 2015; 35: 6619–6629.
5. Basbaum AI, Bautista DM, Scherrer G, et al. Cellular and molecular mechanisms of pain. *Cell* 2009; 139: 267–284.
6. Strassman AM, Raymond SA and Burstein R. Sensitization of meningeal sensory neurons and the origin of headaches. *Nature* 1996; 384: 560–564.
7. Strassman AM and Levy D. Response properties of dural nociceptors in relation to headache. *J Neurophysiol* 2006; 95: 1298–1306.
8. Levy D and Strassman AM. Mechanical response properties of A and C primary afferent neurons innervating the rat intracranial dura. *J Neurophysiol* 2002; 88: 3021–3031.
9. Craig AD. Pain mechanisms: Labeled lines versus convergence in central processing. *Annu Rev Neurosci* 2003; 26: 1–30.
10. Todd AJ. Neuronal circuitry for pain processing in the dorsal horn. *Nat Rev Neurosci* 2010; 11: 823–836.

11. Burstein R, Yamamura H, Malick A, et al. Chemical stimulation of the intracranial dura induces enhanced responses to facial stimulation in brain stem trigeminal neurons. *J Neurophysiol* 1998; 79: 964–982.
12. Malick A, Strassman RM and Burstein R. Trigeminohypothalamic and reticulohypothalamic tract neurons in the upper cervical spinal cord and caudal medulla of the rat. *J Neurophysiol* 2000; 84: 2078–2112.
13. Braz JM, Nassar MA, Wood JN, et al. Parallel "pain" pathways arise from subpopulations of primary afferent nociceptor. *Neuron* 2005; 47: 787–793.
14. Snider WD and McMahon SB. Tackling pain at the source: New ideas about nociceptors. *Neuron* 1998; 20: 629–632.
15. Zhang X, Strassman AM, Novack V, et al. Extracranial injections of botulinum neurotoxin type A inhibit intracranial meningeal nociceptors' responses to stimulation of TRPV1 and TRPA1 channels: Are we getting closer to solving this puzzle? *Cephalalgia* 2016; 36: 875–886.
16. Melo-Carrillo A, Strassman AM, Schain AJ, et al. Exploring the effects of extracranial injections of botulinum toxin type A on prolonged intracranial meningeal nociceptors responses to cortical spreading depression in female rats. *Cephalalgia* 2019; 39: 1358–1365.
17. Burstein R, Zhang X, Levy D, et al. Selective inhibition of meningeal nociceptors by botulinum neurotoxin type A: Therapeutic implications for migraine and other pains. *Cephalalgia* 2014; 34: 853–869.
18. Melo-Carrillo A, Strassman AM, Nir RR, et al. Fremanezumab – a humanized monoclonal anti-CGRP antibody – inhibits thinly myelinated (Adelta) but not unmyelinated (C) meningeal nociceptors. *J Neurosci* 2017; 37: 10587–10596.
19. Melo-Carrillo A, Noseda R, Nir RR, et al. Selective inhibition of trigeminovascular neurons by fremanezumab: A humanized monoclonal anti-CGRP antibody. *J Neurosci* 2017; 37: 7149–7163.
20. Dolly JO and Aoki KR. The structure and mode of action of different botulinum toxins. *Eur J Neurol* 2006; 13: 1–9.
21. Morenilla-Palao C, Planells-Cases R, Garcia-Sanz N, et al. Regulated exocytosis contributes to protein kinase C potentiation of vanilloid receptor activity. *J Biol Chem* 2004; 279: 25665–25672.
22. Aurora SK, Dodick DW, Turkel CC, et al. OnabotulinumtoxinA for treatment of chronic migraine: Results from the double-blind, randomized, placebo-controlled phase of the PREEMPT 1 trial. *Cephalalgia* 2010; 30: 793–803.
23. Silberstein SD, Dodick DW, Bigal ME, et al. Fremanezumab for the preventive treatment of chronic migraine. *N Engl J Med* 2017; 377: 2113–2122.
24. Boudreau GP. Treatment of chronic migraine with erenumab alone or as an add on therapy: A real-world observational study. *Anesth Pain Res* 2020; 4: 1–4.
25. Zhang X, Levy D, Kainz V, et al. Activation of central trigeminovascular neurons by cortical spreading depression. *Ann Neurol* 2011; 69: 855–865.
26. Hansen JM, Lipton RB, Dodick DW, et al. Migraine headache is present in the aura phase: A prospective study. *Neurology* 2012; 79: 2044–2049.
27. Headache Classification Committee of the International Headache Society. The International Classification of Headache Disorders, 3rd edition. *Cephalalgia* 2018; 38: 1–211.
28. Diener HC, Dodick DW, Aurora SK, et al. OnabotulinumtoxinA for treatment of chronic migraine: Results from the double-blind, randomized, placebo-controlled phase of the PREEMPT 2 trial. *Cephalalgia* 2010; 30: 804–814.
29. Rossetto O, Pirazzini M and Montecucco C. Botulinum neurotoxins: Genetic, structural and mechanistic insights. *Nat Rev Microbiol* 2014; 12: 535–549.
30. Dong M, Yeh F, Tepp WH, et al. SV2 is the protein receptor for botulinum neurotoxin A. *Science* 2006; 312: 592–596.
31. Ferrandiz-Huertas C, Mathivanan S, Wolf CJ, et al. Trafficking of thermoTRP channels. *Membranes* 2014; 4: 525–564.
32. Hargreaves R and Olesen J. Calcitonin gene-related peptide modulators – the history and renaissance of a new migraine drug class. *Headache* 2019; 59: 951–970.
33. Hay DL, Garelja ML, Poyner DR, et al. Update on the pharmacology of calcitonin/CGRP family of peptides: IUPHAR Review 25. *Br J Pharmacol* 2018; 175: 3–17.
34. Lipton RB, Croop R, Stock EG, et al. Rimegepant, an oral calcitonin gene-related peptide receptor antagonist, for migraine. *N Engl J Med* 2019; 381: 142–149.
35. Croop R, Goadsby PJ, Stock DA, et al. Efficacy, safety, and tolerability of rimegepant orally disintegrating tablet for the acute treatment of migraine: A randomised, phase 3, double-blind, placebo-controlled trial. *Lancet* 2019; 394: 737–745.
36. Dodick DW, Lipton RB, Ailani J, et al. Ubrogepant, an acute treatment for migraine, improved patient-reported functional disability and satisfaction in 2 single-attack Phase 3 randomized trials, ACHIEVE I and II. *Headache* 2020; 60: 686–700.
37. Goadsby P, Dodick D, Trugman JM, et al. Orally administered atogepant was efficacious, safe, and tolerable for the prevention of migraine: Results from a Phase 2b/3 study. *Neurology* 2019; 92: S17.001.
38. Eftekhari S, Warfvinge K, Blixt FW, et al. Differentiation of nerve fibers storing CGRP and CGRP receptors in the peripheral trigeminovascular system. *J Pain* 2013; 14: 1289–1303.
39. Moreno MJ, Cohen Z, Stanimirovic DB, et al. Functional calcitonin gene-related peptide type 1 and adrenomedullin receptors in human trigeminal ganglia, brain vessels, and cerebromicrovascular or astroglial cells in culture. *J Cereb Blood Flow Metab* 1999; 19: 1270–1278.
40. Zhao J and Levy D. The CGRP receptor antagonist BIBN4096 inhibits prolonged meningeal afferent activation evoked by brief local K(+) stimulation but not cortical spreading depression-induced afferent sensitization. *Pain Rep* 2018; 3: e632.